Phospholipid Reorientation at the Lipid/Water Interface Measured by High Resolution ^{31}P Field Cycling NMR Spectroscopy

Mary F. Roberts,[†*] Alfred G. Redfield,[‡] and Udayan Mohanty[†]
[†]Merkert Chemistry Center, Boston College, Chestnut Hill, Massachusetts; and [‡]Department of Biochemistry, Brandeis University, Waltham, Massachusetts

ABSTRACT The magnetic field dependence of the ^{31}P spin-lattice relaxation rate, R_1, of phospholipids can be used to differentiate motions for these molecules in a variety of unilamellar vesicles. In particular, internal motion with a 5- to 10-ns correlation time has been attributed to diffusion-in-a-cone of the phosphodiester region, analogous to motion of a cylinder in a liquid hydrocarbon. We use the temperature dependence of ^{31}P R_1 at low field (0.03–0.08 T), which reflects this correlation time, to explore the energy barriers associated with this motion. Most phospholipids exhibit a similar energy barrier of 13.2 $\pm$ 1.9 kJ/mol at temperatures above that associated with their gel-to-liquid-crystalline transition (T_m); at temperatures below T_m, this barrier increases dramatically to 68.5 $\pm$ 7.3 kJ/mol. This temperature dependence is broadly interpreted as arising from diffusive motion of the lipid axis in a spatially rough potential energy landscape. The inclusion of cholesterol in these vesicles has only moderate effects for phospholipids at temperatures above their T_m, but significantly reduces the energy barrier (to 17 $\pm$ 4 kJ/mol) at temperatures below the T_m of the pure lipid. Very-low-field R_1 data indicate that cholesterol inclusion alters the averaged disposition of the phosphorus-to-glycerol-proton vector (both its average length and its average angle with respect to the membrane normal) that determines the ^{31}P relaxation.

INTRODUCTION

Phospholipid motions in bilayers can be significantly affected by the inclusion of other components. Although acyl chain motions have been well characterized, the dynamics of the phospholipid phosphate moiety, often critical in interactions with peripheral proteins, are harder to monitor. ^{31}P NMR spectroscopy has been used to measure relaxation behavior of the phosphodiester group in lipid molecules in bilayers. However, at high magnetic fields, large linewidths interfere with this approach. It is quite difficult to identify the combinations of motions reflected in different spectral measurements. Instead, we use high-resolution ^{31}P field cycling NMR spectroscopy (P-fc-NMR) to monitor the field dependence of the ^{31}P spin-lattice relaxation rate (R_1) for diverse phospholipid mixtures over a wide field range (0.003–11.7 T on the same spectrometer) (1,2). For phospholipids aggregated in small unilamellar vesicles, the method extracts three distinct correlation times: a microsecond correlation time, τ_v, an intermediate 5–15 ns time, τ_c, and a short 100–300 ps time, τ_{hf}. The longest of these correlation times reflects vesicle tumbling with some contribution from lateral diffusion, and the shortest time reflects some relatively local dynamics.

Here, we interpret measurements of the intermediate correlation time versus temperature, membrane components, and cholesterol content. Analysis of the dipalmitoylphosphatidylcholine (DPPC) ^{31}P relaxation profile and comparison with molecular dynamics simulations have strongly suggested that the intermediate time, τ_c, which reports the dipolar interaction of the glycerol C(3) protons with the phosphorus, reflects ''wobble in a cone'' of the vectors connecting the phosphorus to the two nearest protons on the glycerol, analogous to motion in a hexadecane-like medium (3). Such wobble reflects motions of the chains, as well as the glycerophosphate moiety. The simulations also suggested that the choline headgroup motions are largely uncoupled from the rest of the phospholipid. For liquid-crystalline-phase bilayers, the temperature dependence of τ_c should reflect a spatially rough potential energy landscape that is similar for different liquid-crystalline systems. A gel-like bilayer should strongly affect the ^{31}P dynamics inherent in τ_c.

We have estimated apparent motional energy barriers for phospholipid τ_c motion in a variety of vesicles and assessed the effect of cholesterol on phospholipid motions. There is a dramatic difference in the barrier for the phospholipid rotational/wobble diffusion in gel (~60 kJ/mol) versus liquid-crystalline (10–15 kJ/mol) states. Bilayer curvature differences of inner and outer leaflets have a significant effect for the anionic phosphatidic acid (PA), but not for zwitterionic PC motion, the latter result suggesting that changes in zwitterionic headgroup packing in the absence of a phase change do not modulate τ_c behavior significantly. The addition of cholesterol can also change the dynamics for the motion reflected in τ_c. Its presence significantly reduces the wobble energy for phosphatidylcholine below the T_m of the pure material, but leads to only a small increase in this energy term for τ_c motions in fluid bilayers. The results are discussed in terms of phospholipid P-H motions suggested by simulations and framed in terms of a rough potential energy landscape.

Submitted January 7, 2009, and accepted for publication March 24, 2009.

*Correspondence: mary.roberts@bc.edu

Editor: J. Antoinette Killian.

0006-3495/09/07/0132/10 $2.00

doi: 10.1016/j.bpj.2009.03.057

MATERIALS AND METHODS

Chemicals and sample preparation

Phospholipids were obtained from Avanti Polar Lipids (Birmingham, AL) and used without further purification. Cholesterol, obtained from Sigma-Aldrich (St. Louis, MO), was recrystallized from ethanol. Small unilamellar vesicles (SUVs) of most lipid combinations were prepared by sonication of lipids rehydrated in 50 mM HEPES, pH 7.5, 20–40% D_2O, 5 mM EDTA. Large unilamellar vesicles (LUVs) of ~1000 Å diameter for DPPC, dimyristoylphosphatidylcholine (DMPC), and DPPC/cholesterol were prepared by extrusion of the lipids in the same buffer using a Lipofast extruder (obtained from Avanti) with a 0.1-μm filter. Samples were epoxied into 8 mM NMR tubes adapted for use with the shuttler (1,4).

^{31}P field cycling (P-fc-NMR)

The ^{31}P spin-lattice relaxation rate (R_1) was measured from 11.7 down to 0.003 T as described previously (1,2,4), but with a modified cycling attachment (see Fig. S1 in the Supporting Material). Samples of 10 mM phospholipid typically required 24–36 h for a full field dependence profile. Deconvolution of the data from 0.07 to 11.7 T to extract τ_c and other parameters that we tabulate followed previously published procedures (1,2,5,6). For samples where the temperature was varied at fixed low field (usually 0.032 T but occasionally other fixed fields as well), measuring R_1 at five or six temperatures typically took 4–8 h.

RESULTS

P-fc-NMR experiment: extracted parameters

Phospholipids in vesicles exhibit similar profiles when the ^{31}P relaxation rate, R_1, is measured from 11.7 down to 0.003 T (1–3). Fig. 1 shows such data for dioleoylphosphatidylethanolamine (DOPE) in SUVs (1:1) with dioleoylphosphatidylmethanol (DOPMe). A detailed review of the different contributions to this profile can be found in Fig. S2. Above 0.05 T (Fig. 1 *A*), there are three distinct terms: 1), dipolar relaxation by the protons closest to the ^{31}P with a timescale of 5–10 ns (τ_c) and extrapolated amplitude at zero field of $R_c(0)$; 2), chemical shift anisotropy (CSA) relaxation with the same correlation time; and 3), a faster motion yielding a CSA term with a 50- to 200-ps correlation time that only contributes significantly above 2 T (1). The extrapolated value of the first (dipolar) term, just mentioned, to the zero field limit, is well determined. From the dipolar τ_c and $R_c(0)$, we can obtain a distance average $\Sigma\langle r^{-3}\rangle^2$, whose inverse sixth root we denote by r_{PH}. The parameters $R_c(0)$ and τ_c are easily estimated from the relaxation rate data (Fig. 1 *A*).

Below 0.05 T (Fig. 1 *B*), another dispersion is seen; this represents dipolar relaxation not averaged by the faster motions and reflects the contribution of vesicle tumbling and lateral diffusion to the ^{31}P R_1 (2). This dispersion is characterized by a correlation time τ_v (typically 0.3–1 μs), and an amplitude $R_v(0)$ (Fig. 1 *B*). On a frequency scale, this very-low-field dispersion is within the range previously suggested (7) for vesicle tumbling from ^{2}H relaxation studies of phospholipids. In that earlier work, it was suggested that vesicle tumbling contributes to relaxation below 10 MHz. Our ^{31}P data indicate that for these small vesicles, that dispersion for vesicle tumbling has a midpoint of ~0.5 Mz. If we assume

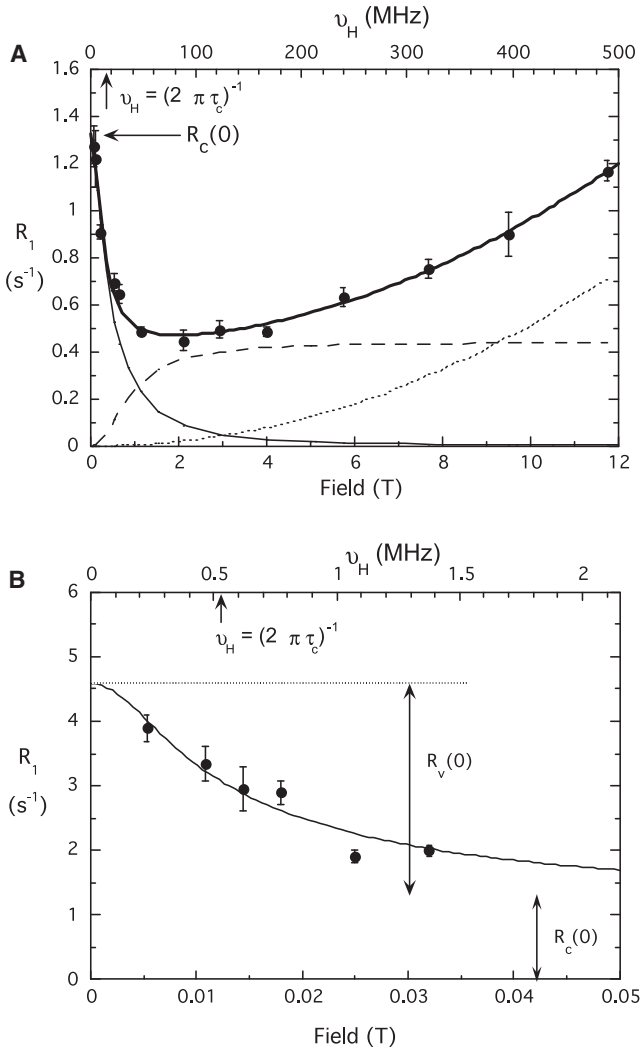

FIGURE 1 (*A*) ^{31}P R_1 for DOPE in mixed vesicles of DOPE (5 mM)/DOPMe (5 mM) from 0.07 to 11.7 T measured at 22°C, showing the theoretically fitted relaxation profile with the individual dipolar (*thin solid line*), CSA (*dashed line*), and high-field CSA associated with faster motion (*dotted line*) components. (*B*) Low-field region obtained in the same run, plotted on an expanded field axis and compressed R_1 axis, showing how the low-field dispersion in R_1 exhibits a 0.3-μs correlation time, due mainly to overall vesicle tumbling (along with lateral diffusion) for DOPE. Also shown in each panel is the ^{1}H frequency scale associated with R_1. The POPMe ^{31}P resonance observed in the same run shows similar behavior, and is omitted here for clarity. The values of $R_c(0)$ and $R_v(0)$ obtained from a computer fit are indicated, to show how those are simply related to amplitude plateaus in the data. Likewise, the field points where the proton angular frequency of $2\pi\upsilon_H$ equals the computer-fitted τ_c^{-1} and τ_v^{-1} are shown to indicate how these correlation times can be estimated directly from the relaxation profiles.

as a model that all the protons producing the relaxation have a P-H vector that is nearly fixed at an angle of θ_{PH} relative to the membrane normal (8), then we can extract an average angle, θ_{PH}, for the P-H vector. Molecular dynamics simulations (3) suggest that of the possible angles from this treatment, the value ~45° appears most plausible for θ_{PH}.

TABLE 1 Correlation times, r_{PH}, θ_{PH}, and E_a for τ_c motion extrapolated from high-resolution ^{31}P field cycling of phospholipids in fluid-phase unilamellar vesicles

Vesicle system*	T (°C)	τ_c † (ns)	$R_c(0)$ (s^{-1})	r_{PH} (Å)	τ_v (μs)	$R_v(0)$ (s^{-1})	θ_{PH} (°)	E_a‡ (kJ/mol)	Energy roughness§ (kJ/mol)
Liquid crystalline									
DOPMe/	22	5.6 ± 1.6	0.92 ± 0.03	2.88	0.54 ± 0.19	4.4 ± 0.5	46.3	10.2 ± 2.5	3.60
POPC¶		5.6 ± 0.6	0.97 ± 0.07	2.85	0.54 ± 0.10	8.4 ± 2.3	43.7	12.0 ± 3.3	3.92
DOPG/	22	4.7 ± 0.7	1.14 ± 0.05	2.70	0.34 ± 0.02	6.1 ± 0.3	44.1	15.6 ± 2.3	4.34
POPC		4.0 ± 0.4	1.03 ± 0.03	2.67	0.40 ± 0.04	8.5 ± 0.6	43.6	13.2 ± 2.4	3.87
DOPMe/	22	27 ± 11	1.48 ± 0.31	3.45	0.58 ± 0.23	2.5 ± 0.9	44.1	13.5 ± 2.3	4.18
DOPE		10.0 ± 1.2	1.33 ± 0.04	2.98	0.30 ± 0.07	3.3 ± 0.5	43.8	13.9 ± 3.1	4.65
DOPA(out)/	22	8.3 ± 2.2	1.37 ± 0.09	2.87	0.53 ± 0.19	6.8 ± 1.1	44.1	10.5 ± 2.3	3.56
DOPA(in)/		21.7 ± 6.0	3.05 ± 0.40	2.95	1.04 ± 0.50	7.0 ± 0.9	46.3	27.4 ± 3.7	5.64
POPC		8.8 ± 3.2	1.50 ± 0.14	2.86	0.46 ± 0.17	8.0 ± 1.0	42.7	13.0 ± 2.0	3.92
POPC+Pr^{3+}(out)/	22	1.6 ± 0.1	1.39 ± 0.13	–	0.37 ± 0.12	6.8 ± 1.4	–	22.4 ± 4.0	5.15
POPC(in)		7.2 ± 1.6	1.62 ± 0.14	2.73	0.44 ± 0.09	8.4 ± 1.1	43.5	14.0 ± 3.1	4.16
DMPC SUVs	30	7.6 ± 0.9	1.44 ± 0.37	2.81	0.94 ± 0.18	19.1 ± 2.4	42.4	16.1 ± 3.3	3.95
DPPC LUVs	45	11.2 ± 2.4	1.39 ± 0.07	3.02					
SPM SUVs	40	13.8 ± 2.8	3.45 ± 0.26	2.68				31.1 ± 7.8	6.52
DOPMe/	37	15.2 ± 4.5	1.38 ± 0.15	3.18	0.54 ± 0.18	3.3 ± 0.9	44.8	18.9 ± 5.4	5.99
SPM		9.2 ± 4.2	1.59 ± 0.18	2.85	0.65 ± 0.14	8.5 ± 1.6	44.2	14.3 ± 3.6	4.51
Gel-like:									
DMPC SUVs								62 ± 23	8.69
DPPC LUVs								67.2 ± 6.8	7.71
SPM (w/DOPMe)								76.5 ± 13.5	9.55

*For SUVs, R_1 was measured between 0.003 and 11.7 T at the indicated temperature and the $R(0)$ parameters were extracted from that field dependent profile.

†The fit of R_1 versus field to extract $R_c(0)$ and τ_c was usually carried out with data from 0.08 to 11.7 T.

‡The activation energy was evaluated from the slope of the plot of ln(R_1 at fixed low field) versus $1/T$; data for at least five temperatures were acquired (usually between 17 and 45°C).

§The root-mean-squared energy roughness was evaluated from the square root of slope of the plot of ln(R_1) versus $1/T^2$.

¶Data from Roberts and Redfield (1).

The parameters τ_c, $R_c(0)$, r_{PH}, τ_v, $R_v(0)$, and θ_{PH} are presented in Table 1. The phospholipid rotational/wobble diffusion reflected in τ_c is of particular interest, since it is likely to vary with phospholipid mixtures and phase states. A temperature dependence of τ_c would help us describe the energetics of each component in mixed phospholipid vesicles. Since the timescales τ_c and τ_v are well separated, we can extract an energy term for τ_c by measuring how R_1 varies with temperature but at fixed low field, where it is expected to be directly proportional to τ_c.

Mixed component SUVs: temperature dependence of τ_c

SUVs composed of 1-palmitoyl-2-oleoylphosphatidylcholine (POPC) (10 mM) and DOPMe (10 mM) have been previously studied at 22°C by high-resolution ^{31}P field cycling (1,2). At a field of 0.032 T, the relaxation rate is essentially $R_c(0)$, which is directly proportional to τ_c, as just mentioned. The temperature dependence of R_1 for this vesicle system is shown in Fig. 2. If we assume that over the temperature range studied, no other motion adds a significant component to R_1, that the P-O-C-H angle with respect to the bilayer normal does not change significantly with temperature, and that at a field strength of 0.032 T, R_1 does indeed reflect $R_c(0)$ over the same temperature range, then the apparent activation energy, E_a, associated with this motion is 12.0 ± 3.3 kJ/mol for POPC and 10.2 ± 2.5 kJ/mol for DOPMe. The E_a extracted for both phospholipids in these vesicles is relatively small. For comparison, an E_a extracted from the temperature dependence of hexadecane viscosity (9), thought to be a mimic of the bilayer interior, is 15.4 kJ/mol.

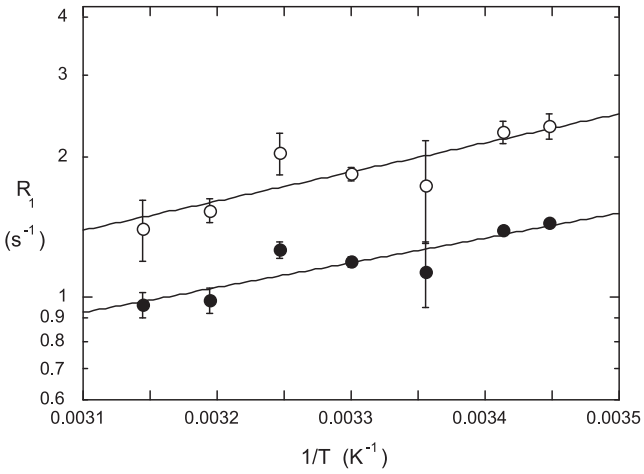

FIGURE 2 Temperature dependence of R_1 measured at 0.032 T for SUVs composed of 10 mM POPC (○) and 10 mM DOPMe (●).

Other SUVs composed of zwitterionic and anionic phospholipids above their phase transition temperatures were also examined (Table 1). POPC and dioleoylphosphatidylglycerol (DOPG) yield results very similar to the POPC/DOPMe system, as expected if chain motions and the overall internal viscosity contribute significantly to the motion implicit in τ_c. The combination of DOPE/DOPMe exhibited an increase in the τ_c for DOPMe, as well as longer r_{PH}, compared to the corresponding values observed for that anionic lipid mixed with POPC. Such behavior is consistent with a change in the glycerol/headgroup orientation of the anionic lipid when PE replaces PC. However, Table 1 shows that the E_a values for each lipid in the different fluid phase vesicles (Table 1) are not statistically different from each other or from those of the PC/anionic phospholipid mixtures.

Effect of vesicle curvature on phospholipid dynamics

A particularly interesting mixed-vesicle system is the SUV composed of dioleoylphosphatidic acid (DOPA) and POPC at pH 7.5. In these small, highly curved vesicles, the pK_a for formation of the PA dianion on the inner monolayer is dramatically increased (>10), so that it is a monoanion, whereas the PA on the outer surface exhibits a net charge controlled by buffer, in this case 0.05 M Tris HCl, pH 8.0 (10). This leads to distinct chemical shifts for the PA in the two leaflets. For POPC/DOPA vesicles at 22°C (Fig. 3 *A*), both PC and PA in the outer leaflet have similar τ_c values (8.8 ± 3.2 and 8.3 ± 2.2 ns, respectively), whereas the τ_c for PA on the inner layer has increased to 21.7 ± 6.0 ns (Table 1). The effective r_{PH} is similar for all three lipids, consistent with the *sn*-3 glycerol proton(s) dominating the τ_c relaxation of each phosphorus nucleus (1). Analysis of the very low field region indicates similar $R_v(0)$ values for the two PA resonances but a longer τ_v for the PA on the inner monolayer (Table 1), the latter reflecting a reduced lateral diffusion contribution to this dipolar relaxation. The similar $R_v(0)$ and increased τ_v does indicate that the PA on the inner monolayer has a different (increased) average θ_{PH}, the angle made by the P-H vector with the bilayer normal (2). Perhaps more interesting is the temperature dependence of R_1 (Fig. 3 *B*). Values extrapolated for E_a are similar for POPC and DOPA on the outer monolayer (13.0 ± 2.0 and 10.5 ± 2.3 kJ/mol, respectively). However, E_a for the PA packed in the inner leaflet of these SUVs is significantly increased (27.4 ± 3.7 kJ/mol). Presumably, the tighter packing of the PA monoanion on the inner leaflet restricts the ^{31}P motion contributing to τ_c.

The results for the POPC/DOPA SUVs might suggest that vesicle curvature has a strong effect on motion and orientation of the phospholipid headgroup. However, that inference is complicated by the fact that the PA on the inner monolayer has an altered net charge and likely a different averaged θ_{PH} in the membrane compared to PA in the outer leaflet of the SUV. For POPC SUVs, the chemical shift of the external leaflet PC can be separated from the inner leaflet by the addition of a lanthanide ion. Pr^{3+} (3 mM in excess of the 1 mM EDTA) added to 20 mM POPC SUVs shifts the outer leaflet PC peak ~7 ppm downfield, well removed from the inner leaflet PC resonance. The PC on the inner leaflet of the vesicle has a τ_c of 7.2 ± 1.6 ns, similar to the τ_c for PC in vesicles in the absence of Pr^{3+} (Table 1). The R_1 temperature dependence for this peak gives E_a = 14.0 ± 3.1 kJ/mol, a value comparable to that seen for SUVs dominated by external PC. In contrast to PA in the inner leaflet, the motion of PC in the inner leaflet of these highly curved vesicles is not significantly restricted in terms of τ_c. Therefore, the markedly hindered motions and energetics seen with PA on the inner leaflet of SUVs reflect that particular molecule, and do not occur for the zwitterionic lipid PC on the inner leaflet.

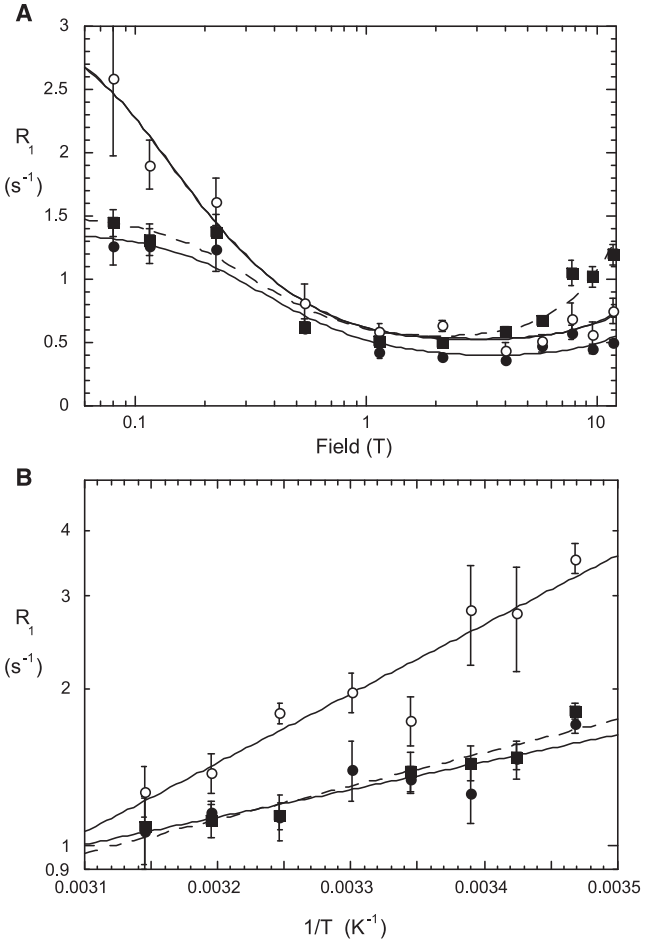

FIGURE 3 (*A*) Variation of R_1 from 0.07 to 11.7 T for POPC (□), DOPA on the outer monolayer (●), and DOPA on the inner monolayer (○) in SUVs (5 mM each phospholipid) at 22°C. (*B*) Temperature dependence of R_1 at 0.08 T for POPC (■) and DOPA on the outer (●) and inner (○) monolayers.

Influence of phospholipid phase state on E_a

The phase state of the bilayer is another property that should have a strong effect on the effective rotation/wobbling of phospholipids in a bilayer. We chose two different saturated

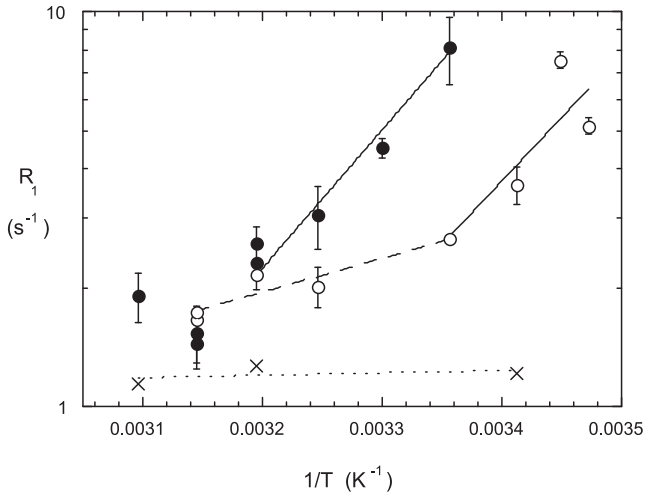

FIGURE 4 Temperature dependence of R_1 at 0.032 T for DPPC (•) and DMPC LUVs (○). The solid lines show the fit for gel-state PC, whereas the dashed line shows the fit for liquid-crystalline DMPC. Also shown is R_1 at 11.74 T for DPPC LUVs (X).

chain PC species: DPPC examined in LUVs and DMPC in SUVs. DPPC has a T_m of ~41°C, whereas DMPC has a T_m of ~26°C. Instrumental limitations meant we could study the gel state of DPPC, but could not obtain enough data for its liquid-crystalline state. However, the DMPC SUVs could be examined both above and below the T_m. As shown in Fig. 4, for DMPC, the log(R_1) versus 1/T at 0.032 T had a lower slope above the T_m compared to that below it. For the gel-state DPPC, the temperature dependence of R_1 (values for $T < 40$°C) led to an energy of 67.2 ± 6.8 kJ/mol. For DMPC ($T < 26$°C), a similar energy term was obtained, 62 ± 23 kJ/mol. The large error is in part due to the instability of the SUVs below the T_m, which leads to fusion over the course of a day and loss of signal intensity, so that relatively short relaxation experiments were used. For comparison, the E_a for liquid-crystalline DMPC was 16.1 ± 3.3 kJ/mol. It is clear that packing the lipids in a gel state dramatically impedes wobble and rotational diffusion of the phospholipids in the membrane.

For comparison, the effect of temperature on R_1 for DPPC at 11.7 T over the same temperature range (which includes both liquid crystalline and gel phases) was examined. There was very little change in R_1 over the temperature range, and the apparent E_a from an Arrhenius plot was 5.2 ± 4.2 kJ/mol. The value is not interpretable, because it has contributions from CSA mechanisms.

The same technique can be applied to binary lipid vesicles for which there is a temperature at which one component, by itself, would be in a liquid-crystalline phase and the other, by itself, would be in a gel state. To explore this, we examined SUVs containing both DOPMe and sphingomyelin (SPM). When it is pure, bovine SPM has a somewhat broadened but distinct transition from a gel-like to a liquid-crystalline state in the temperature range 30–35°C. This transition temperature is likely to be reduced in SUVs with an equal proportion of a liquid-crystalline lipid, in this case DOPMe. At 37°C, where both components are in a fluid, liquid-crystalline phase, τ_c is 9.2 ± 4.2 ns for SPM and 15.2 ± 4.5 ns for DOPMe. At a fixed low field (0.032 T), R_1 increases as the temperature decreases (Fig. 5). However, unlike the components of the other binary vesicles, the Arrhenius plot for the SPM component is biphasic, with a much steeper slope below 25°C (Fig. 5 *B*). There is only a small increase in the slope for the PMe component of the vesicle in the same temperature region (Fig. 5 *A*). For data above 25°C, the E_a values for DOPMe (18.9 ± 5.4 kJ/mol) and SPM (14.3 ± 3.6 kJ/mol) in the fluid phase were similar to values for other liquid-crystalline components (Table 1). However, in the low temperature regime, the two energy terms were significantly different: E_a = 76.5 ± 13.5 kJ/mol for SPM and 29.0 ± 5.8 kJ/mol for DOPMe. Presumably, the higher value for SPM represents the energy barrier for gel-like SPM in local SPM-enriched regions, whereas the DOPMe shows smaller changes. The rotation/wobble is not impeded nearly as much for DOPMe, which is not below its T_m when pure,

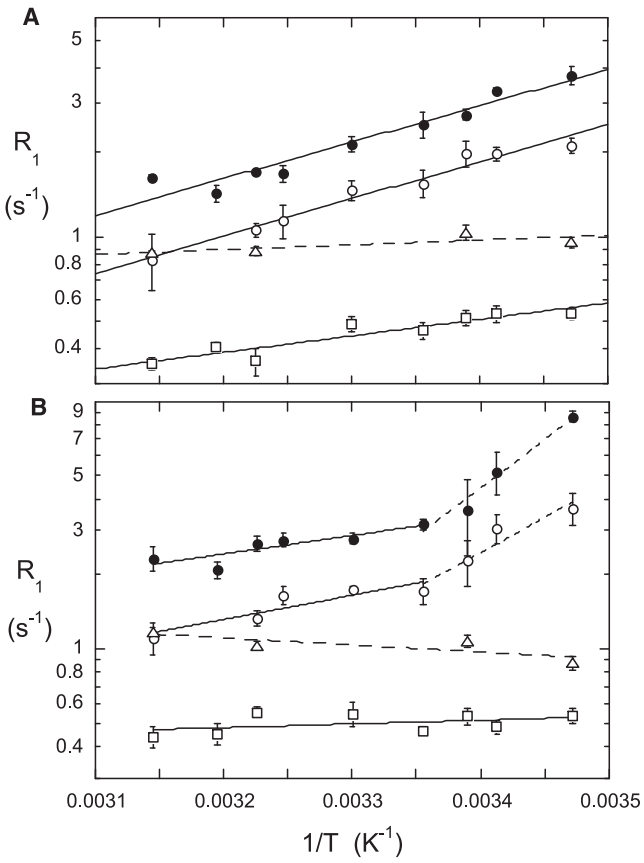

FIGURE 5 Temperature dependence of ^{31}P R_1 for vesicles composed of 1:1 (*A*) DOPMe and (*B*) SPM measured at 0.032 (•), 0.115 T (○), 2.13 T (□), and 11.74 T (△). Note that the PMe data at each field strength can be fit by a single exponential versus inverse temperature. For SPM where the R_1 is measured in a regime dominated by the dipolar τ_c, the dependence is biphasic, with a higher slope (larger E_a) for SPM in a gel-like state.

TABLE 2 Correlation times, *R*(0) values, and extracted parameters for phospholipids in vesicles containing 30 mol % cholesterol

Lipids	T (°C)	$R_c(0)$ (s^{-1})	r_{PH} (Å)	τ_c (ns)	$R_v(0)$ (s^{-1})	τ_v (μs)	θ_{PH}	E_a* (kJ/mol)	Energy roughness (kJ/mol)
POPC	22	1.87 ± 0.28	3.24	23.3 ± 8.0	6.37 ± 0.60	0.46 ± 0.06	39.8	15.3 ± 1.5	4.33
DPPC†	45	2.71 ± 0.14	3.43	47.3 ± 5.4				21.0 ± 4.1	6.04
DMPC†	45	1.74 ± 0.13	3.47	32.5 ± 6.4				11.7 ± 3.0	3.82
SPM†	40	2.06 ± 0.56	3.53	43 ± 18				2.6 ± 0.4	1.80
POPC/	22	1.67 ± 0.23	3.35	25.3 ± 7.1	6.22 ± 0.34	0.50 ± 0.09	39.3	15.1 ± 1.4	
DOPMe		1.48 ± 0.19	3.30	20.3 ± 6.1	2.62 ± 0.17	0.33 ± 0.09	42.5	17.1 ± 0.9	
POPC/	40	1.16 ± 0.10	3.49	22.6 ± 9.5	5.94 ± 0.15	0.45 ± 0.04	37.1	15.1 ± 1.4	4.35
DOPMe		0.83 ± 0.10	3.36	12.7 ± 4.5	2.98 ± 0.08	0.49 ± 0.04	43.2	17.9 ± 0.8	4.82
DPPC/	25	2.75 ± 0.16	3.34	40.8 ± 5.1				13.1 ± 1.0	4.09
DOPMe		1.96 ± 0.06	3.14	20.3 ± 1.5				14.9 ± 2.3	4.35

*Extrapolated from the temperature dependence of R_1 at 0.032 T.
†The very low field increase in R_1 for LUVs with cholesterol could not be determined with sufficient accuracy to obtain $R_v(0)$ or τ_v, precluding an estimation of θ_{PH}.

as for SPM below 25°C, although there is some effect. The sensitivity of the R_1 temperature dependence to partial phase separation is only observed at fixed low fields where dipolar relaxation is dominant (Fig. 5 *B*).

In summary, from an examination of these different SUV systems where both gel and liquid-crystalline phases can coexist, we see that chain packing (and presumably bilayer viscosity) plays a significant role in modulating the motion reflected in the ^{31}P τ_c. The mean E_a for gel-phase PC and SPM is 68.6 ± 4.2 kJ/mol; above the T_m, the mean E_a for PC is 13.7 ± 0.7 kJ/mol.

Effects of cholesterol on phospholipid dynamics

Cholesterol in bilayers is said to "fluidize" a gel-state phospholipid bilayer and to slow down motions in a liquid-crystalline bilayer. We examined these effects in three different types of vesicles: 1), saturated chain PC/cholesterol (30 mol %) vesicles; 2), binary component SUVs with PC/DOPMe/cholesterol (10 mM/35 mM/30 mM) where the PC was either POPC or DPPC; and 3), SPM/cholesterol (20 mM/10 mM) LUVs. The cholesterol-containing vesicles with DPPC or SPM were prepared by extrusion to have a diameter of ~1000 Å. Table 2 compares relaxation parameters extracted from the field cycling experiments.

Cholesterol dramatically increased the POPC τ_c, from 5 ns in fluid-phase bilayers at 22°C, in the absence of the sterol, to 23 ns with cholesterol added. Vesicles of DPPC (or DMPC) above their T_m showed a similar increase in τ_c with cholesterol. For example, Fig. 6 shows the effect of cholesterol on DPPC ^{31}P R_1 field dependence at 45°C. The shift in the curve, such that the midpoint of the R_1 rise occurs at lower field, is the hallmark of the increased τ_c. At a temperature where the PC in a pure or binary component vesicle is above its T_m, the addition of 30 mol % cholesterol led to a 4.4 ± 0.2-fold increase in τ_c (Table 2). The effect on $R_c(0)$ was much smaller (a 1.7 ± 0.3-fold increase). Added cholesterol has the result of substantially increasing r_{PH} for phospholipids: r_{PH} increased from 2.85 to 3.35 Å for PC and from 2.88 to 3.30 Å for PMe. Since the glycerol C(3)H_2 group most likely provides the major dipolar relaxation, this indicates that the averaged arrangement of the P-O-C(3)H_2 has been changed by the cholesterol.

For both POPC/cholesterol and POPC/DOPMe/cholesterol vesicles, θ_{PH} decreased significantly for the PC component

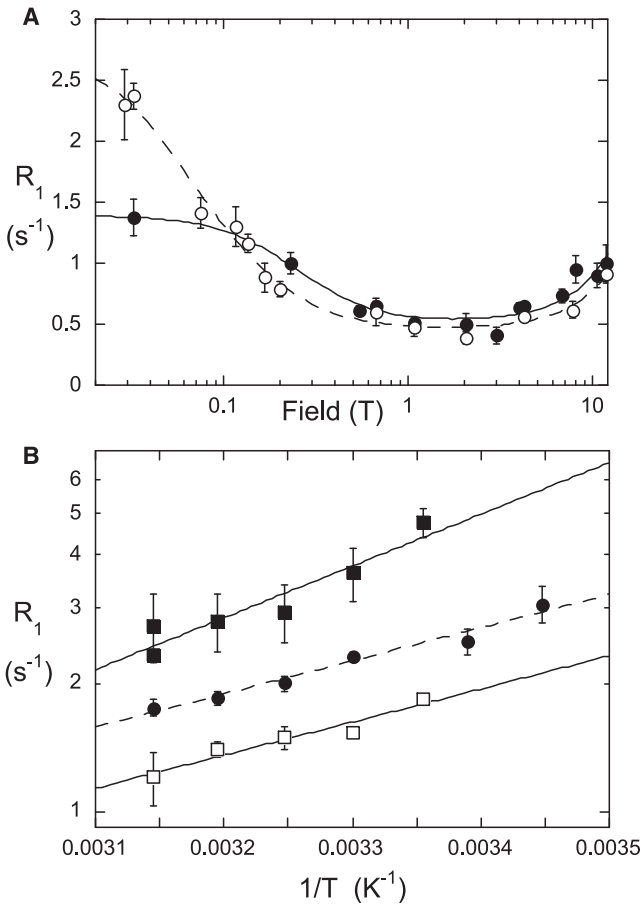

FIGURE 6 (*A*) Field dependence (at 45°C) of R_1 from 0.03 to 11.7 T for DPPC (•) and DPPC (○) in the presence of 30 mol % cholesterol. Note the large increase in τ_c in the presence of cholesterol along with a smaller increase in $R_c(0)$. (*B*) Temperature dependence of R_1 measured at 0.032 T for vesicles with 30 mol % cholesterol in POPC SUVs (•), DPPC LUVs (■), and DPPC/DOPMe (1:1) SUVs (□).

(an average of 4°) with a smaller reduction in the averaged angle for PMe (1.7° decrease). These results complement previous ^{31}P NMR studies of how cholesterol affects the ^{31}P of PC (11), where there was no change in the chemical shift anisotropies with up to 50 mol % cholesterol. That observation was used to suggest that cholesterol does not order the headgroup as it does the hydrocarbon region; rather, it acts as a spacer. The τ_c we measured clearly shows that the dipolar motions relaxing the phosphorus are retarded and that the P-H angle with respect to the bilayer normal is altered with cholesterol added.

The E_a for the POPC internal wobble/rotation motion from the temperature dependence of R_1 was only marginally affected by the presence of cholesterol. The average E_a for POPC in pure or binary-component SUVs in the absence of cholesterol was 13.0 ± 0.8 kJ/mol; this value was 14.5 ± 1.2 kJ/mol when cholesterol was present. DOPMe in mixed vesicles exhibited a slightly larger (and statistically significant) increase in E_a with cholesterol, from 11.9 ± 2.3 to 16.0 ± 1.6 kJ/mol. However, the most dramatic change was for saturated-chain PC vesicles where E_a was evaluated at temperatures below the T_m of the pure lipid. Best illustrated for DPPC LUVs with cholesterol (Fig. 6 *B*), E_a was reduced from 67.2 ± 6.8 kJ/mol to 21.0 ± 4.1 kJ/mol. Likewise, data for DMPC LUVs no longer exhibited a biphasic R_1 versus $1/T$ profile but could be fit with a single exponential yielding 11.7 ± 3.0 kJ/mol with the sterol present. The one outlier was the SPM/cholesterol LUV sample, where τ_c at 40°C (43 ± 10 ns) was similar to that observed for DPPC at 45°C (47.3 ± 5.4 ns), but the E_a extrapolated for SPM was much lower (2.6 ± 0.4 kJ/mol).

Brownian motion theory

Relation of R_1 temperature dependence to the local energy landscape

Previously, we compared our data for DPPC with the results of a computer simulation (3). Here, we present an alternative view to assess the energetics of phospholipids in vesicles, using modern Brownian motion theory. We suggest that features of the wobble motion could be analyzed as diffusive motion of the lipid axis in a spatially rough potential energy landscape.

The phospholipid wobble can be considered as Brownian motion of the lipid axis in the energy landscape predominantly along a single reaction coordinate x. The motion of the phosphorus-glycerol chain unit, viewed as a rigid body of mass m, is assumed to be described by a one-dimensional Smoluchowski equation (see Fig. S3 for details and references supporting this theory). We assume that diffusion in the gel state takes place in a spatially rough energy landscape. Initially, as a possible approximation to the gel state, we assume that the potential energy landscape $\Phi(x)$ along the reaction coordinate x is random. The average of the potential over the realization of $\Phi(x)$ is denoted by $\langle V(x)\rangle$. The fluctuations of the potential along the reaction coordinate is by definition $\delta\ \Phi(x) = \Phi(x) - \langle V(x)\rangle$. Let the correlation between the fluctuations at two points, x and y, on the energy landscape be given by $\langle \delta\ \Phi(x)\ \delta\Phi\ (y)\rangle = \Gamma\ (x - y)$.

A quantity of interest is the mean first-passage time, $\tau(x)$, for the system starting at x to reach a domain Ω for the first time. This quantity will be averaged over the probability distribution that defines the random potential $\Phi(x)$. If the fluctuations in the potential are Gaussian, one obtains (see Fig. S3)

$$\ln\langle\tau\rangle\ =\ \ln R_1\ =\ \Gamma(0)/\left(k_B^2T^2\right)\ +\ \ln\tau_o, \qquad (1)$$

where $\Gamma(0)$ is not a function of temperature, the angular brackets denote an average over the probability distribution, and τ_o is a characteristic timescale.

Several comments are in order. First, the first term in this expression has a characteristic $1/T^2$ temperature dependence that arises from the roughness in the energy landscape (12,13). Second, the temperature dependence of the term $\ln\tau_o$ is the product of viscosity of the fluid and an activation energy. By fitting Eq. 1 to our data for the temperature dependence of R_1, we have compiled in Table 1 values for root-mean-squared energy roughness for phospholipids in vesicles. Viewing the experimental data through this analysis indicates that phospholipids in liquid-crystalline bilayers have a similar root-mean-squared energy roughness (4.07 ± 0.12 kJ/mol for PC and 3.92 ± 0.20 kJ/mol for anionic phospholipids in SUVs with PC, with the exception of PA in the inner monolayer of SUVs) and τ_o (since the E_a values are all quite similar). Third, inclusion of cholesterol in fluid bilayers will likely increase the $\ln\tau_o$ term, but its effect on the root-mean-squared roughness of the energy landscape may not be as dramatic. Experimentally, we see that the effect on the root-mean-squared roughness of the energy landscape is relatively small, with an average value of 4.15 ± 0.12 kJ/mol (except in the SPM sample). This value is not statistically different from the value in the absence of cholesterol. However, for all these lipids, the overall τ has increased, as is reflected in the τ_o term, consistent with an increased viscosity. The gel-state bilayers examined have both a steeper roughness (8.65 ± 0.53 kJ/mol) and an increased τ_o term. Inclusion of cholesterol in these bilayers reduces both terms. For DPPC, the root-mean-squared roughness of the energy landscape is decreased to 6.04 kJ/mol, a decrease of ~30%, whereas the ln τ_o term exhibits a much larger decrease when the activation energy is examined.

The model described above for the first passage time is based on two assumptions. The first is the validity of the Smoluchowski equation, which is obtained from the more fundamental Langevin equation under conditions of high friction, γ, using projection operator and perturbation techniques. The second assumption is that the potential average energy does have a small value along x, and this would act like a barrier. This assumption can be relaxed. As mentioned

before, the rough potential can be thought of as having a background potential that is smooth over a suitable length scale, Δx, and on which is overlaid a random perturbation. There is another length scale in the problem, namely the amplitude, ϑ, of the random perturbation. Provided there is separation between these two length scales, using mean first-passage time formalism, the diffusion coefficient in a rough potential will be significantly depressed over that in a uniform potential by a term proportional to $e^{-(\vartheta/k_BT)^2}$. This approach to describing the energy landscape of phospholipids in a vesicle emphasizes the similarity of individual components of fluid bilayers and provides a framework for describing how additives affect the bilayer components.

Relation of apparent energy barriers to heat capacity

Here, we show that there is an intimate connection between the slope of the temperature dependence of R_1 for the gel-state lipid, with and without the presence of cholesterol, and the heat capacity of the system. This idea was motivated by two previous observations (14,15). Firstly, for DPPC and DMPC LUVs, the temperature dependence of heat capacity near the gel-liquid-crystalline phase change can be described by critical exponents (14). Fluctuations at the critical point lead to divergence in measurable thermodynamic properties such as heat capacity and compressibility as one approaches the critical point, and can be described by scaling laws. Secondly, there is a relationship between the relaxation kinetics of lipid membranes and heat capacity (15).

Consider a thermodynamic fluctuation in the system whose magnitude is $\Delta\chi$. According to Landau-Lifshitz fluctuation theory, the probability that fluctuation will occur in the gel-lipid system is given by

$$P(\Delta\chi) = \left(2\pi\langle(\Delta\chi)^2\rangle\right)^{-1/2}\exp\left(-\frac{1}{2}\frac{(\Delta\chi)^2}{\langle(\Delta\chi)^2\rangle}\right), \quad (2)$$

where χ denotes the driving force. The driving force is related to fluctuations in appropriate thermodynamic quantities (see Fig. S4). If, at a given temperature and pressure, the magnitude of the fluctuations are below a threshold value, then the probability of occurrence of these fluctuations is such that it would greatly suppress molecular rearrangements. Thus, if the driving force corresponding to the threshold fluctuations is less than a minimum value, $\Delta\chi^*$, the system cannot relax to equilibrium (16).

For a fluctuation in the system that is large enough to allow a transition, the probability per unit time, or the transition probability, for such a fluctuation is given by $\int_{\Delta\chi^*}^{\infty} d(\Delta\chi)P(\Delta\chi)$. The relaxation time, τ, is, however, inversely proportional to the transition probability. We now introduce an order parameter that describes the gel state of the DPPC and DMPC bilayers. Assuming that the driving force that leads to relaxation is due to entropy (16), we can show that the temperature dependence of the relaxation time can be expressed as

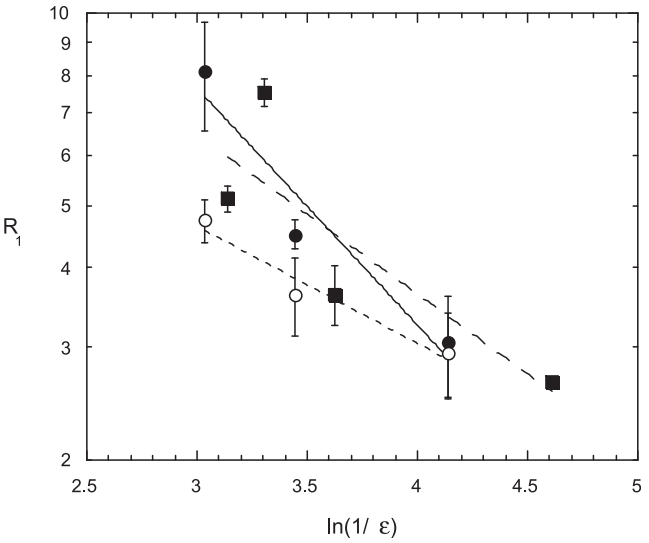

FIGURE 7 Dependence of $\ln(R_1)$ obtained at 0.032 T on $\ln(1/\varepsilon)$, where $\varepsilon = (T_c - T)/T_c$ for both DPPC LUVs (•), DMPC SUVs (■), and DPPC/cholesterol LUVs (○). For DMPC, the T_c extracted from the data was 28°C; for DPPC (in the absence and presence of 30 mol % cholesterol), a T_m of 40°C was used to estimate ε.

$$\ln\tau \approx \text{const} - \frac{(\alpha + \beta)}{2}\ln(1/\varepsilon), \quad (3)$$

where $\varepsilon = (T_c - T)/T_c$, T_c is the critical temperature equal to T_m, α and β are exponents that define the constant-volume heat capacity and the order parameter near the phase change, respectively. Thus, the relaxation time, which in these experiments is proportional to R_1 at a low field, where τ_c dominates the motion, has a term proportional to the heat capacity raised to the power $\alpha/2$.

Fig. 7 shows such a plot of $\ln(R_1)$ (at 0.032 T, this is proportional to τ_c) versus $\ln(1/\varepsilon)$ for both DPPC and DMPC bilayers below the T_m, where the T_m for DPPC is 40°C and that for DMPC is 28°C. Data for DPPC with 30 mol % cholesterol is also shown, assuming that 40°C still represents the T_m. The magnitude of the slope, equivalent to $(\alpha + \beta)/2$, is 0.85 ± 0.25 for DPPC and 0.60 ± 0.30 for DMPC. Although the values for $(\alpha + \beta)$ are slightly higher than expected, they are fairly close to the expected range within the error of the measurement. A lower slope, 0.42 ± 0.10, is observed for the DPPC sample containing cholesterol. These values are consistent with the temperature dependence of the τ_c for the ^{31}P group of the phospholipid, reflecting changes in the heat capacity of the gel-like phase.

DISCUSSION

^{31}P E_a estimates: past, present, and what affects it

The field dependence of the ^{31}P spin-lattice relaxation rates of phospholipids in bilayers can provide insights into the motions of this region of the molecule and how overall

phospholipid motion is affected by different conditions. The similarity of E_a (13.2 ± 1.9 kJ/mol for glycerophospholipids in fluid bilayers, irrespective of headgroup) and the energy roughness extrapolated from it in almost all phospholipid vesicles, small or large, pure components or mixtures of phospholipids, suggests that what governs the τ_c motion is the same for almost all of these samples. Assuming that τ_c is correlated with wobbling of the P-glycerol-chain cylinder in a hexadecane-like environment (3), as molecular dynamics simulations suggest, such uniformity would be expected (along with similar roughness in the potential energy landscape). There are two previous estimates of energy barriers from ^{31}P NMR studies that are similar to what we see, although motions characterized by those estimates were not clearly identified. Measurements of egg PC vesicles at four fields (down to 2.26 T) and several temperatures generated an apparent E_a of 16.9 kJ/mol (17). Dufourc et al. (18) examined unoriented and aligned DMPC with a wide variety of ^{31}P NMR experiments and differentiated several types of motions over a wide temperature range. They estimated an energy barrier of 15 kJ/mol for headgroup rotation of DMPC in the liquid-crystalline phase that increased to 50 kJ/mol for the gel state; the latter value is similar to what we measure for PC (64.6 ± 2.6 kJ/mol). It is clear that the phospholipid phase state has a very large effect on the energy barrier associated with τ_c.

The only situation where E_a for a component of a fluid bilayer was statistically different from 13 kJ/mol was for DOPA on the inner monolayer of highly curved vesicles. Both τ_c and E_a indicate that wobbling/rotation of inner-monolayer DOPA is relatively difficult. There are several possible mechanisms to explain the slower motion for inner-monolayer PA. Since the PA in this leaflet has a much higher pK_a, the net charge/molecule is −1 (10). This could allow closer packing of PA molecules, potentially in microdomains that do not mix well with the POPC that also is packed in the inner monolayer. Since we cannot differentiate the PC in these bilayers (Pr^{3+} added to SUVs with anionic phospholipids causes fusion), we do not know how the motion of that lipid is affected, although we only see a single exponential for decay of PC magnetization in R_1 experiments.

Insights into cholesterol effects

Cholesterol incorporated in a phospholipid bilayer leads to very interesting effects as measured by P-fc-NMR. There appears to be a change in the averaged orientation and effective distance of the P-H vector that is responsible for the dipolar relaxation of the phosphorus. These changes in both r_{PH} (lengthened) and θ_{PH} (angle increased) are statistically significant and suggest 1), a real alteration in phospholipid average headgroup geometry in the presence of cholesterol; 2), a further uncoupling of the polar headgroup motions from the phosphorus such that they no longer have much contribution to R_1; or 3), a breakdown in the rigid body model for phospholipid motion in a bilayer such that the phosphate unit is partially uncoupled from the glycerol/acyl chain behavior in a way that reduces the effectiveness of the glycerol C(3) proton dipolar interactions. There is little in the literature that addresses ^{31}P headgroup changes in bilayers containing cholesterol (an earlier study suggested that changes in CSA did not occur (11)). At this time, we cannot decide which of these possibilities is correct (although the breakdown in the rigid body model seems least likely, since a dramatically lengthened τ_c is observed) without extensive molecular dynamics simulations and further studies of systems with perdeuterated moieties. However, the field cycling opens the possibility of really defining what happens around the phosphorus in these bilayers.

One of the most striking changes is that in the presence of cholesterol, the E_a associated with τ_c for bilayers, at temperatures where the pure phospholipids would be gel-like, is dramatically reduced. Presumably, this is because at 30 mol %, the cholesterol disrupts the ordered-chain packing (acting as a spacer (11)) that retards the wobble diffusion sensed by τ_c. Analyses of ^{2}H NMR spectra have suggested that cholesterol affected order fluctuations rather than local segmental motions (19). Nonetheless, the temperature dependence of τ_c in these bilayers still reflects fluctuations in the heat capacity of the saturated phospholipid as the T_m is approached, since the magnitude of the slope of $\ln(R_1)$ versus $\ln(1/\varepsilon)$ is ~0.5. For fluid bilayers, τ_c increases fourfold when cholesterol is included, whereas the increase in E_a is relatively small (for PC in vesicles, E_a increases from 13 to 15 kJ/mol). The value is not at all like that in gel-state bilayers, and is not even as high as for PA in the inner leaflet in SUVs. The roughness of the energy landscape as interpreted by the theory presented has also been seen to decrease with cholesterol present. Calorimetric studies have shown that inclusion of cholesterol broadens the melting transition, and this loss of cooperative behavior is reflected in the energetics of τ_c in cholesterol-containing bilayers in the temperature regime below the T_m.

Cholesterol and saturated-chain PC have been noted to form ''condensed complexes'' (20,21). In a recent work, Lee and co-workers (22) presented evidence for PC/cholesterol ordering that persists only over a few molecules. Such behavior is consistent with dynamic PC/cholesterol complexes. The size mismatch of phospholipid tails and the cholesterol tail means the complex cannot be fully ordered but should rather exhibit short-range ordering. Contrary to this view, Lindblom and co-workers (23) suggested that the formation of coexisting liquid ordered and disordered phases does not require one to invoke specific phospholipid-cholesterol complexes, since cholesterol partitions into both phases. Is there any evidence in our work for discrete complexes? The average τ_c for DMPC and DPPC with cholesterol at 45°C is 40 ± 7 ns; for POPC, in similar cholesterol-containing vesicles, the average τ_c is 23 ns at 22°C and extrapolated to be 15 ns at 45°C. This behavior

might support the idea that a tighter and more constrained complex is formed for saturated-chain PC than for the POPC complexes. We can estimate that for τ_c to increase to 40 ns, all else being the same, the POPC/cholesterol SUVs would have to be at 7°C. It is interesting to note that if one looks at the T_m for pure POPC bilayers, one gets an average of -1.4 ± 1.0°C (http://www.lipidat.ul.ie/search.htm). Thus, the POPC bilayers with cholesterol ~7–8° above the T_m for the pure lipid are projected to be the same as those for DPPC with cholesterol at 45°C, a temperature ~5° above the T_m for the pure lipid. By adjusting for reduced temperature of the pure lipid, we might suggest that the observation of differential cholesterol complexes with saturated versus unsaturated PC reflects interactions based on the relative fluidity of the chains rather than a specific complex with a saturated-chain PC. Although further studies are clearly warranted, this does highlight that using high-resolution field cycling, very useful information can be extracted that is not easily obtainable from other techniques.

SUPPORTING MATERIAL

Nine equations are available at http://www.biophysj.org/biophysj/supplemental/S0006-3495(09)00844-3.

We thank Dr. Rich Pastor for insightful discussions.

This research was supported by National Science Foundation MCB-0517381 (to M.F.R.), and by National Institutes of Health GM 077974 (to A.G.R.).

REFERENCES

1. Roberts, M. F., and A. G. Redfield. 2004. High-resolution ^{31}P field cycling NMR as a probe of phospholipid dynamics. *J. Am. Chem. Soc.* 126:13765–13777.
2. Roberts, M. F., and A. G. Redfield. 2004. Phospholipid bilayer surface configuration probed quantitatively by ^{31}P field-cycling NMR. *Proc. Natl. Acad. Sci. USA.* 101:17066–17071.
3. Klauda, J. B., M. F. Roberts, A. G. Redfield, B. R. Brooks, and R. W. Pastor. 2008. Rotation of lipids in membranes: MD simulation, ^{31}P spin-lattice relaxation, and rigid-body dynamics. *Biophys. J.* 94:3074–3083.
4. Redfield, A. G. 2003. Shuttling device for high-resolution measurements of relaxation and related phenomena in solution at low field, using a shared commercial 500 MHz NMR instrument. *Magn. Reson. Chem.* 41:753–768.
5. Roberts, M. F., Q. Cui, C. J. Turner, D. A. Case, and A. G. Redfield. 2004. High-resolution field-cycling NMR studies of a DNA octamer as a probe of phosphodiester dynamics and comparison with computer simulation. *Biochemistry.* 43:3637–3650.
6. Lipari, G., and A. Szabo. 1982. Model-free approach to the interpretation of nuclear magnetic resonance relaxation in macromolecules. 1. Theory and range of validity. *J. Am. Chem. Soc.* 104:4546–4559.
7. Halle, B. 1991. 2H NMR relaxation in phospholipid bilayers. Toward a consistent molecular interpretation. *J. Phys. Chem.* 95:6724–6733.
8. Woessner, D. E. 1962. Nuclear spin relaxation in ellipsoids undergoing rotational Brownian motion. *J. Chem. Phys.* 37:647–654.
9. Small, D. M. 1986. The Physical Chemistry of Lipids: From Alkanes to Phospholipids, 2nd ed. Springer, New York. 568–570.
10. Swairjo, M. A., B. A. Seaton, and M. F. Roberts. 1994. Effect of vesicle composition and curvature on the dissociation of phosphatidic acid in small unilamellar vesicles: a ^{31}P NMR study. *Biochim. Biophys. Acta.* 1191:354–361.
11. Brown, M. F., and J. Seelig. 1978. Influence of cholesterol on the polar region of phosphatidylcholine and phosphatidylethanolamine bilayers. *Biochemistry.* 17:381–384.
12. Zwanzig, R. 1988. Diffusion in a rough potential. *Proc. Natl. Acad. Sci. U.S.A.* 85:2029–2030.
13. De Gennes, P. G. 1975. Brownian motion of a classical particle through potential barriers: Application to the helix-coil transitions of heteropolymers. *J. Stat. Phys.* 12:463–481.
14. Nagano, H., H. Yao, and K. Ema. 1995. Dynamic heat capacity at the gel to liquid-crystalline phase transition in large unilamellar vesicles of dimyristoylphosphatidylcholine in the ultralow frequency region. *Phys. Rev. E.* 51:3363–3367.
15. Grabitz, P., V. P. Ivanova, and T. Heimburg. 2002. Relaxation kinetics of lipid membranes and its relation to heat capacity. *Biophys. J.* 82: 299–309.
16. Gordon, J. M. 1978. A derivation of temperature dependence of the relaxation times of glass-forming liquids. *J. Phys. Chem.* 82:963–965.
17. Milburn, M. P., and K. R. Jeffrey. 1987. Dynamics of the phosphate group in phospholipid bilayers. *Biophys. J.* 52:791–799.
18. Dufourc, E. J., C. Mayer, J. Stohrer, G. Althoff, and G. Kothe. 1992. Dynamics of phosphate head groups in biomembranes. Comprehensive analysis using phosphorus-31 nuclear magnetic resonance lineshape and relaxation time measurements. *Biophys. J.* 61:42–57.
19. Martinez, G. V., E. M. Dykstra, S. Lope-Piedrafita, C. Job, and M. F. Brown. 2002. NMR elastometry of fluid membranes in the mesoscopic regime. *Phys. Rev. E.* 66:050902.
20. Radhakrishnan, A., and H. M. McConnell. 1999. Condensed complexes of cholesterol and phospholipids. *Biophys. J.* 77:1507–1517.
21. Radhakrishnan, A., and H. M. McConnell. 2003. Condensed complexes of cholesterol and phospholipids. *Biochim. Biophys. Acta.* 1610: 159–173.
22. Ege, C., M. K. Ratajczak, J. Majewski, K. Kjaer, and K. Y. C. Lee. 2006. Evidence for lipid/cholesterol ordering in model lipid membranes. *Biophys. J.* 91:L01–L03.
23. Lindblom, G., G. Oradd, and A. Fillippov. 2006. Lipid lateral diffusion in bilayers with phosphatidylcholine, sphingomyelin and cholesterol. An NMR study of dynamics and lateral phase separation. *Chem. Phys. Lipids.* 141:179–184.